Improvement of thickness uniformity and elements distribution homogeneity for multicomponent films prepared by coaxial scanning pulsed laser deposition technique

Juguang Hu (胡居广), Qiwen Li (李启文), Xiaodong Lin (林晓东)*, Yi Liu (刘 毅), Jinghua Long (龙井华), Liuyang Wang (王刘杨), and Huabin Tang (汤华斌)

College of Physics Science and Technology, Shenzhen University, Shenzhen 518060, China

**Corresponding author: linxd@szu.edu.cn*

Received November 27, 2013; accepted April 29, 2014; posted online June 25, 2014

In conventional pulsed laser deposition (PLD) technique, plume deflection and composition distribution change with the laser incident direction and pulse energy, then causing uneven film thickness and composition distribution for a multicomponent film and eventually leading to low device quality and low rate of final products. We present a novel method based on PLD for depositing large CIGS films with uniform thickness and stoichiometry. By oscillating a mirror placed coaxially with the incident laser beam, the laser's focus is scanned across the rotating target surface. This arrangement maintains a constant reflectance and optical distance, ensuring that a consistent energy density is delivered to the target surface by each laser pulse. Scanning the laser spot across the target suppresses the formation of micro-columns, and thus the plume deflection effect that reduces film uniformity in conventional PLD technique is eliminated. This coaxial scanning PLD method is used to deposit a CIGS film, 500 nm thick, with thickness uniformity exceeding ±3% within a 5 cm diameter, and exhibiting a highly homogeneous elemental distribution.

OCIS codes: 220.0220, 220.4830, 310.0310, 310.1860.

doi: 10.3788/COL201412.072201.

Pulsed laser deposition (PLD) is a powerful and versatile technique for growing films of a wide range of materials. It is especially suitable for depositing multicomponent films such as YBCO (usually $YBa_2Cu_3O_{6+x}$) superconductor films[1,2] or CIGS (usually $CuIn_{0.7}G_{0.3}S_2$) films for solar cells[3], or $La_{0.7}Sr_{0.3}Mn_{0.5}Fe_{0.5}O_3$ (LSMFO) thin films[4]. However, film thickness and elements distribution inhomogeneities in multicomponent films lead to band-gap fluctuations, which have a detrimental effect on the device performance[5−9]; thus, maintaining a high level of uniformity of both thickness and stoichiometry is crucial, especially for large area films produce or experiments.

Unfortunately, ensuring such spatial uniformity with conventional PLD techniques is complicated by interactions between the laser and the target material. The composition, structural quality, surface roughness, and optical band gap value of the film may be affected by variations in the intensity of the incident laser. This is because the spatial distributions of the plume and the species it carries change as a function of laser fluence[10]. The plume is characterized by a highly polar, forward-peaked distribution, which results in thickness inhomogeneity for large-area films[11]. During conventional deposition, the target and substrate are rotating and the ablated spot is stationary with respect to the axis of the rotating substrate; over long periods of irradiation, micro-columns form on the target surface, which cause the plume to deflect towards the incident beam[12]. This effect makes it difficult to predict the final film thickness and contributes to inhomogeneity of the thickness and the local ratio of atomic species.

To obtain films with uniform thickness, a number of techniques have been introduced: rotational/ translational PLD and offset PLD[13,14]; the matrix-assisted pulsed laser evaporation (MAPLE) technique[15,16]; inverse pulsed laser deposition (IPLD)[17]; the shadow-mask technique[18]; dynamic deposition configuration[19]; the multi-beam approach[20]. Unfortunately, these techniques present various drawbacks, such as inefficient use of target materials, low deposition rate, difficulties in preparing large-area films, and increased complexity. In this letter we report a PLD configuration, designed to allow the straightforward deposition of large, homogeneous films; we name the method coaxial scanning PLD (CSPLD).

In this configuration (Fig. 1), the axis of the scanning mirror is coaxial with the direction of incident laser beam. The plane of the mirror is tilted with respect to the beam, such that the laser is reflected at a glancing angle onto the target in the vacuum chamber. As the axis of the mirror oscillates, the mirror changes its normal direction, and the laser spot is scanned back and forth across the surface of the target.

The principle behind this configuration is illustrated in Fig. 2. The angle α between the incident laser beam and the mirror remains constant during scanning, as does the position of the laser spot on the mirror, which ensures that the reflectance does not vary. This avoids energy variations in the reflected non-polarized laser pulse as the mirror oscillates. Assuming the incident laser direction (or, equivalently, the rotating axis of the mirror) is

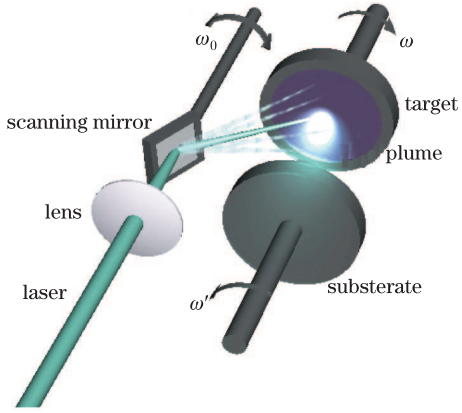

Fig. 1. (Color online) Schematic diagram of the CSPLD experimental set-up.

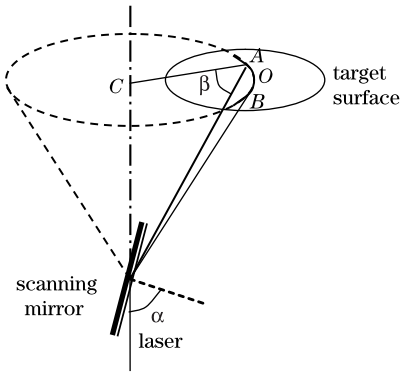

Fig. 2. The geometry of the CSPLD configuration. The laser spot tracks back and forth along the arc AOB on the target surface as the mirror oscillates.

perpendicular to the plane of the target surface, the incident angle β between the laser and the target surface is kept constant. The geometry also ensures that the distance from the focus lens to the laser spot on the target does not change during the deposition process. Thus, the laser fluence on the target surface is the same for each pulse, regardless of the orientation of the scanning mirror.

The incident angle α of laser beam on the mirror is set to be larger than 45° to make the beam focus on the target in such a way as to keep the laser fluence (energy density) constant. The track followed by the laser focal spot during scanning is the arc AOB in Fig. 2. We assume that the axes of substrate and target are collinear. In order to obtain a film with uniform thickness, a correspondingly larger amount of plasma must be deposited at larger radial distances from the center. One way to achieve this is varying the scanning speed of the laser so that it spends more time near the outer edge of the target than at the center, while maintaining a fixed pulse frequency[13]. The speed of the laser spot along the arc AOB is thus set to be slowest near the target center O, and fastest near the target edge (points A and B). The laser spot speed v is varied according to

$$v(r) = kr^{-n}, \tag{1}$$

where r is the radial distance from the center of the target, and the exponent n is approximately 1; the optimal values of n and the coefficient k for ensuring film thickness homogeneity are determined experimentally. An alternative way to obtain uniform thickness is by varying the laser pulse repetition rate and the corresponding deposition time at each location on the target[12]. In this approach, the laser beam is scanned along the target at a constant speed, and the pulse repetition rate is increased as a function of radial distance[21].

The CIGS films preparation experiments were carried out in a vacuum chamber with a basic pressure of 5×10^{-4} Pa. The films were grown using a KrF laser (λ=248 nm) to ablate rotating CIGS ceramic targets 5 cm in diameter; the resulting plasma was deposited on quartz substrates with the same size at 500 °C. The laser fluence was set to be 5 J/cm^2 with a repetition rate of 10 Hz. The incident angle at the scanning mirror was α=62.5°, resulting in a laser-target incidence angle of β=35°. The separation between the target and substrate surfaces was 40 mm. Before deposition, the substrates were cleaned sequentially in acetone, alcohol, and deionized water for 10 min each using a Kerry Ultrasonic Bath, and then dried in pure nitrogen gas. A covering straight blade was placed along the diameter of the substrate to make a step for measuring the film thickness[19]. For comparison, a film was prepared by the conventional method as well, to illustrate the influence of plume deflection on the thickness. In this case the substrate was not rotated during the deposition process. Film thickness profiles for the finished films were measured by a profilometer (Surfcorder ET-4000M, Kosaka Laboratory Ltd., Japan), and their atomic composition profiles were measured using energy dispersive spectrometer (EDS) on field emission scanning electron microscope (FESEM, S4700, Hitachi, Japan).

The thickness profiles for films deposited using both conventional PLD and the new CSPLD method are shown in Fig. 3. The thickness distribution of the sample prepared by conventional static PLD is seen to be far from uniform[22,23], dropping to as low as 10% of the maximum value near the film edge; while the film deposited using CSPLD exhibits near-perfect uniformity at all radial positions, maintaining an absolute thickness of about 500 nm. The thickness at the outer edges of the film is slightly lower than that at the center, which can be attributed to the target and substrate having the same diameter and collinear axes of rotation. Thickness uniformity could thus be improved even further by using an off-axis setup and/or a larger target[24].

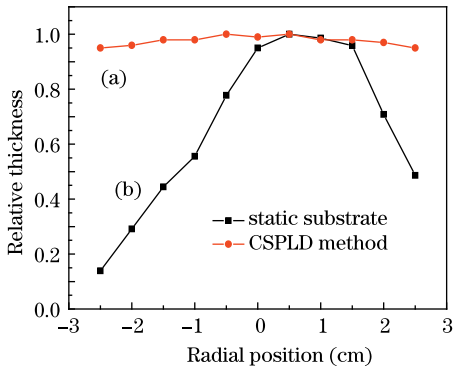

Fig. 3. (Color online) Films thickness distribution profiles for (a) the CSPLD method and (b) the static substrate/static laser spot deposition method.

Figure 4 shows the atomic percentage of Cu, In, Ga, and Se at different radial positions for the two films. The distribution of atomic species is significantly more uniform in the film prepared via (a) the CSPLD method than that prepared via (b) the conventional method. The uniformity is not perfect-the atomic percentage of the lighter species is slightly enhanced at the edge of the film, while heavier ones are somewhat depleted there. This is related to the angular distribution of elements in the plume[25]; it has been shown that lighter Cu species have a broader distribution than the heavier In species[26], and thus the atomic distribution near the film edge is skewed towards lighter species.

A known drawback of conventional PLD is the formation of micro-columns on the target surface, which tend to deflect the plume and thus contribute to inhomogeneities in the deposited film. There have been many attempts to understand the formation of micro-columns, and to compensate for plume deflection[22], but so far none have been successful in suppressing the formation of the micro-columns and eliminating the deflection of the plume. A strong advantage of our CSPLD method is that it does suppress micro-column formation. We propose the following mechanism for this suppression. As explained in Ref. [22], small irregularities on the target surfaces tend to be ablated in a non-uniform way, with the face oriented perpendicularly to the incident beam experiencing the highest local fluence and thus the highest ablation rate. In our novel configuration, the laser spot scans along the target surface, following the track marked AOB in Fig. 2. As the target rotates, a small irregularity will sometimes encounter the laser beam near point A, and sometimes near point B; in each case, it presents a different face to the laser, so over time the irregularity is evenly ablated and micro-columns do not form. Accordingly, the direction of the plume does not deviate during the entire deposition process.

In the conventional PLD geometry, the laser beam irradiates the target along a circular strip as the target is rotated. The direction of the plume slowly deflects towards the direction of the incoming laser, and the symmetry of the plume is also reduced. The plume deflection effect is demonstrated in Fig. 5, which shows a sequence of images taken of the plume during a static substrate/static laser spot PLD process. The plume deviation and asymmetry become more and more pronounced over time.

When the plume expands, there is a preferential propagation of heavy atoms along the normal axis of the plume, which means heavy atoms are enriched at its center[13,23]. Plume deflection over time can thus result in inhomogeneous deposition of atomic species. By suppressing plume deflection, the CSPLD method should enhance stoichiometric uniformity in the film. Our novel configuration ensures the sputtering plume remains perpendicular to the target surface, and should maintain a consistent distribution of mass and atoms in each plume over the deposition process. We speculate that films prepared via CSPLD may have better stoichiometric uniformity than those prepared by other modified PLD methods, as a strong correlation exists between the thickness distribution and the compositional distribution[13]. Further experiments are needed to verify this.

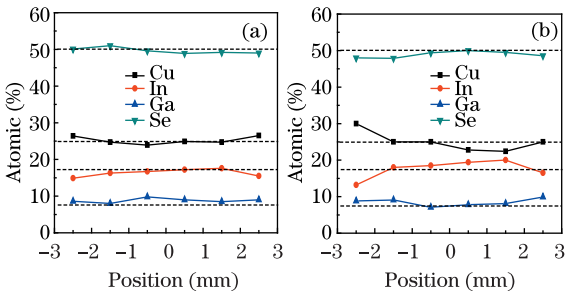

Fig. 4. (Color online) Atomic percentage of Cu, In, Ga, and Se in the film prepared (a) by CSPLD method and (b) by the static substrate/static laser spot deposition method. The dashed line is the nominal percentage.

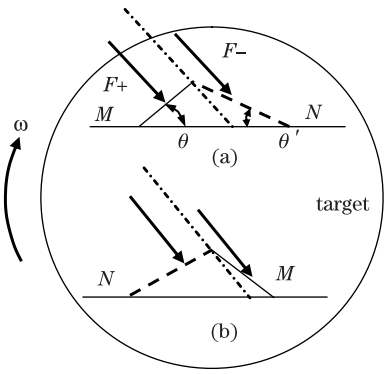

Fig. 5. Schematic drawing illustrating the mechanism for suppressing the formation of micro-columns on the target surface. (a) The laser spot at one side of the target center, and (b) the laser spot moves to another side of the target center. The height of the micro-columns can not increase by the alternate ablation from each side.

In conclusion, we prepare a CIGS film with highly uniform thickness and elemental composition using the CSPLD method. This experimental configuration delivers an identical magnitude of laser energy to the target with each laser pulse, and suppresses the formation of micro-columns on the target surface, thereby eliminating plume deflection. We successfully deposit a CIGS film with a thickness of 500 nm and thickness uniformity better than ±3%, spanning a 5 cm diameter. We propose a mechanism by which the scanning of the laser spot across the target surface in CSPLD suppresses micro-column formation.

This work was supported by the Shenzhen Basic Research Project of Science and Technology under Grant No. JCYJ20120613112423982.

References

1. H. Palonen, H. Huhtinen, and P. Paturi, Thin Solid Films **519,** 8058 (2011).
2. K. Develos-Bagarinao, H. Yamasaki, J. C. Nie, and Y. Nakagawa, Supercond. Sci. Tech. **18,** 667 (2005).
3. P. Jackson, D. Hariskos, E. Lotter, S. Paetel, R. Wuerz, R. Menner, W. Wischmann, and M. Powalla, Prog. Photovolt Res. Appl. **19,** 894 (2011).
4. Y. H. Jo, B. C. Mohanty, and Y. S. Cho, Appl. Sur. Sci. **256,** 6819 (2010).
5. J. J. Yang, R. Wang, W. Liu, Y. Sun, and X. N. Xiao, J. Phys. D Appl. Phys. **42,** 215305 (2009).

6. A. S. Kindyak, V. V. Kindyak, and V. F. Gremenok, Mat. Lett. **28,** 273 (1996).
7. T. Nakada and S. Shirakata, Sol. Energ. Mat. Sol. C **95,** 1463 (2011).
8. C. D. R. Ludwig, T. Gruhn, C. Felser, T. Schilling, J. Windeln, and P. Kratzer, Phys. Rev. Lett. **105,** 025702 (2009).
9. H. Qi, M. Zhu, W. Zhang, K. Yi, H. He, and J. Shao, Chin. Opt. Lett. **10,** 013104 (2012).
10. S. Venkatachalam and Y. Kanno, Curr. Appl. Phys. **9,** 1232 (2009).
11. J. M. Lackner, Sur. Coat. Technol. **200,** 1439 (2005).
12. N. Pryds, J. Schou, and S. Linderoth, Appl. Surf. Sci. **253,** 8231 (2007).
13. M. Fukutomi, K. Komori, K. Kawagishi, and K. Togano, Phys. C **357-360,** 1342 (2001).
14. J. A. Greer and M. D. Tabat, J. Vac. Sci. Technol. A **13,** 1175 (1995).
15. A. Piqué, R. A. McGill, D. B. Chrisey, D. Leonhardt, T. E. Mslna, B. J. Spargo, J. H. Callahan, R. W. Vachet, R. Chung, and M. A. Bucaro, Thin Solid Films **355-356,** 536 (1999).
16. D. B. Chrisey, A. Piquè, R. A. McGill, J. S. Horwitz, and B. R. Ringeisen, Chem. Rev. **103,** 553 (2003).
17. L. Égerházi, Zs. Geretovszky, T. Szörényi, and F. Bari, Appl. Sur. Sci. **257,** 5324 (2011).
18. C. Chen, P. P. Ong, and H. Wang, Thin Solid Films **382,** 275 (2001).
19. D. Guido, L. Cultrera, and A. Perrone, Surf. Coat. Tech. **180-181,** 603 (2004).
20. W. Biegel, R. Klarmann, B. Stritzker, B. Schey, and M. Kuhn, Appl. Surf. Sci. **168,** 227 (2000).
21. N. Pryds, B Toftmann, J. B. Bilde-Sørensen, and S. Linderoth, Appl. Surf. Sci. **252,** 4882 (2006).
22. L. Cultrera, M. I. Zeifman, and A. Perrone, Phys. Rev. B **73,** 075304 (2006).
23. J. Schou, Appl. Surf. Sci. **255,** 5191 (2009).
24. C. V. Varanasi, K. D. Leedy, D. H. Tomich, and G. Subramanyam, Thin Solid Films **517,** 2878 (2009).
25. X. Ni, K. K. Anoop, M. Bianco, S. Amoruso, X. Wang, T. Li, M. Hu, and Z. Song, Chin. Opt. Lett. **11,** 093201 (2013).
26. T. C. Droubay, L. Qiao, T. C. Kaspar, M. H. Engelhard, V. Shutthanandan, and S. A. Chambers, Appl. Phys. Lett. **97,** 124105 (2010).